Defence Research and Development Canada
Recherche et développement pour la défense Canada

DEFENCE R&D DÉFENSE

Detection of aircraft by high frequency sky wave radar under auroral clutter-limited conditions

R. J. Riddolls

Defence R&D Canada – Ottawa
Technical Memorandum
DRDC Ottawa TM 2008-336
March 2009

Canada

Detection of aircraft by high frequency sky wave radar under auroral clutter-limited conditions

R. J. Riddolls
Defence R&D Canada – Ottawa

Defence R&D Canada – Ottawa
Technical Memorandum
DRDC Ottawa TM 2008-336
March 2009

Principal Author

Original signed by R. J. Riddolls

R. J. Riddolls

Approved by

Original signed by D. Dyck

D. Dyck
Head/Radar Systems Section

Approved for release by

Original signed by P. Lavoie

P. Lavoie
Head/Document Review Panel

Abstract

This memorandum describes some of the rudimentary considerations for operating a high frequency sky wave radar in Canada for aircraft detection. A simple macroscopic model of the ionosphere is examined, and the elevation and range resolution limits of a high frequency radar are computed. Limits on azimuth and Doppler resolving capabilities of a radar arise from the presence of plasma density irregularities in the ionospheric propagation path. Scattering from the aurora is quantified using Thomson scattering theory and reasonable agreement with the experimental values of radar cross section can be found in the case of 1-percent plasma density fluctuations. However, the auroral scatter is sufficiently large to prevent detection of small aircraft with radar cross sections of 10 to 20 dBm^2. Combining receive-side adaptive processing with adaptive elements on the transmit side allows the targets to be detected.

Résumé

Le présent document décrit certaines considérations rudimentaires visant l'exploitation d'un radar HF à ondes ionosphériques au Canada aux fins de la détection d'aéronefs. Un modèle macroscopique simple de l'ionosphère est examiné, et les limites de résolution en site et en distance d'un radar HF sont calculées. Les limites des capacités de résolution azimutale et Doppler d'un radar HF tiennent à la présence d'irrégularités dans la densité du plasma sur le trajet de propagation ionosphérique. La diffusion aurorale est quantifiée selon la théorie de diffusion de Thomson. Nous trouvons un bon accord avec les valeurs expérimentales de la surface équivalente radar (SER) dans le cas de fluctuations de densité de 1 pour cent. Toutefois, la SER aurorale est assez grande pour empêcher la détection de petits aéronefs dont la SER va de 10 à 20 dBm^2. En combinant le traitement adaptatif côté réception avec éléments adaptatifs côté émission, on peut détecter les cibles.

This page intentionally left blank.

Executive summary

Detection of aircraft by high frequency sky wave radar under auroral clutter-limited conditions

R. J. Riddolls; DRDC Ottawa TM 2008-336; Defence R&D Canada – Ottawa; March 2009.

This memorandum describes some of the rudimentary considerations for operating a high frequency sky wave radar in Canada for aircraft detection. A simple macroscopic model of the ionosphere is examined, and the elevation and range resolution limits of a high frequency radar are computed. It is shown that the vertical inhomogeneity of the ionosphere causes a radar transmit beam to spread in elevation. However, this elevation spread is far less in extent than what can be resolved by practical radar systems. With regard to range resolution, the ionosphere causes wideband radar pulses to spread in ground range. If this ground range spreading exceeds the radar range resolution, then performance is degraded. This effect places practical limits on the radar waveform bandwidth.

The limits on azimuth and Doppler resolving capabilities of a radar arise from the presence of plasma density irregularities in the ionospheric propagation path. It is found that for an assumption of 1-percent fluctuation levels in the propagation medium, the phase fronts incident on a linear array have a fluctuation level on the order of 10 radians and a correlation distance of about 600 m along the array. This limits azimuth resolving capability to about 1 degree at 10 MHz. The limit on Doppler resolution is determined by invoking the Taylor hypothesis, which supposes that temporal variations in the ionosphere are due to drifting spatial structure. At a nominal drift rate of 100 m/s, the Doppler spreading is about 0.05 Hz.

Scattering from the aurora is quantified using Thomson scattering theory and there is reasonable agreement with the experimental values of radar cross section in the case of 1-percent density fluctuations. However, the auroral radar cross section is sufficiently large to prevent detection of small aircraft with radar cross sections of 10 to 20 dBm^2. Combining receive-side adaptive processing with adaptive elements on the transmit side allows the targets to be detected.

Sommaire

Detection of aircraft by high frequency sky wave radar under auroral clutter-limited conditions

R. J. Riddolls; DRDC Ottawa TM 2008-336; R & D pour la défense Canada – Ottawa; mars 2009.

Le présent document décrit certaines considérations rudimentaires visant l'exploitation d'un radar HF à ondes ionosphériques au Canada aux fins de la détection d'aéronefs. Un modèle macroscopique simple de l'ionosphère est examiné, et les limites de résolution en site et en distance d'un radar HF sont calculées. Le document montre que l'inhomogénéité verticale de l'ionosphère produit un étalement en site du faisceau d'émission radar. Toutefois, cet étalement est bien moins étendu que l'étalement qui peut être résolu par des systèmes radar pratiques. En ce qui concerne la résolution en distance, l'ionosphère produit un étalement en distance topographique des impulsions radar à large bande. Si cet étalement dépasse la résolution en distance du radar, les performances sont dégradées. Cet effet impose des limites pratiques à la largeur de bande des ondes radar.

Les limites des capacités de résolution azimutale et Doppler d'un radar HF tiennent à la présence d'irrégularités dans la densité du plasma sur le trajet de propagation ionosphérique. On a établi, en supposant des niveaux de fluctuation de 1 pour cent dans le milieu de propagation, que des fronts d'ondes incidents sur un réseau linéaire présentaient une fluctuation de l'ordre de 10 radians et, le long du réseau, une distance de corrélation d'environ 600 m. Cela limite la capacité de résolution azimutale à environ 1 degré à 10 MHz. La limite de la résolution Doppler est déterminée par l'hypothése de Taylor, qui suppose que les variations temporelles dans l'ionosphére sont dues à une dérive de la structure spatiale. Pour une dérive nominale de 100 m/s, l'étalement Doppler est d'environ 0,05 Hz.

La diffusion aurorale est quantifiée selon la théorie de diffusion de Thomson. Nous trouvons un bon accord avec les valeurs expérimentales de la surface équivalente radar (SER) dans le cas de fluctuations de densité de 1 pour cent. Toutefois, la SER aurorale est assez grande pour empêcher la détection de petits aéronefs dont la SER va de 10 à 20 dBm^2. En combinant le traitement adaptatif côté réception avec éléments adaptatifs côté émission, on peut détecter les cibles.

Table of contents

This page intentionally left blank.

1 Introduction

High Frequency (HF) sky wave radar uses the ionosphere as a reflecting surface to provide illumination of targets beyond the line-of-sight horizon of the earth [1]. Operation of sky wave radar in Canada is more challenging than in countries at more southern latitudes because of the presence of ionospheric clutter from the earth's auroral zone [2].

Echoes from aircraft are normally Doppler-shifted with respect to ground clutter, and can be detected against noise. However, auroral clutter is spread in Doppler and results in clutter-limited aircraft detection. To be detectable, the target Radar Cross Section (RCS) should be on the order of 10 dB larger than the RCS of the aurora. The aurora RCS is determined primarily by the volume of the radar resolution cell multiplied by the aurora RCS per unit volume. Fine-resolution radars will suffer lower clutter levels than coarse-resolution radars. In the clutter-limited detection scenario, one is thus largely concerned with optimizing radar resolution.

Chapter 2 describes the optimization of the elevation angle resolution and range resolution. The achievable resolution in elevation angle is related to the steepness of the ionization profile of the lower side of the ionosphere. As the ionization profile becomes more gradual, the reflecting properties of the ionosphere become less ideal, which lead to a spreading of the incident radar signal in elevation angle. With regard to range resolution, the ionosphere causes wideband radar pulses to spread in ground range. If this ground range spreading exceeds the radar range resolution, then performance is degraded. This effect places practical limits on the radar waveform bandwidth.

Chapter 3 looks at the limits of the achievable azimuth angle resolution and Doppler resolution. Achievable resolution in these dimensions is more difficult to determine as it depends on the nature of fine-scale irregularities in the ionospheric plasma density. Statistical characterization of these irregularities is available from rocket and satellite measurements [3, 4].

Having computed bounds on the resolving power of the HF radar, in Chapter 4 we turn to a computation of the RCS of the aurora per unit volume. The mechanism of Thomson scattering is described, and the predicted value of RCS per unit volume is compared with results from experiments [2]. A total RCS is then computed by multiplying the minimum radar resolution cell volume determined in Chapters 2 and 3 by the aurora RCS per unit volume.

In Chapter 5, we examine the role of radar clutter that enters the radar data through the sidelobes of the radar beampattern. This contribution can be controlled by adaptive processors when the clutter exhibits spatial correlation across antenna elements or temporal correlation across temporal samples [5]. We examine the performance

of both receive-side and transmit-side adaptive processors using a simple correlation function for the clutter.

2 Resolution In Elevation Angle and Range

The inhomogeneous and dispersive properties of the ionosphere impose limits on the available elevation angle and range resolving power of an HF radar. To keep the complexity of derivations to an absolute minimum we assume an unmagnetized model of the ionospheric plasma and consider a plane-stratified bottomside ionosphere with a linear ionization profile.

2.1 The Radar Signal Trajectory

In the unmagnetized model of the ionosphere, the dispersion relation for electromagnetic waves is given by [6]

$$N^2 = \frac{c^2 k^2}{\omega^2} = 1 - \frac{\omega_p^2}{\omega^2}. \tag{1}$$

Here, N is the index of refraction, ω is the wave frequency, c is the speed of light, k is the wavenumber, and ω_p is the plasma frequency, defined as

$$\omega_p^2 = \frac{e^2 n}{\epsilon_0 m}, \tag{2}$$

where e is the electron charge, n is the number of ionized electrons per unit volume (the "plasma density"), ϵ_0 is the permittivity of free space, and m is the electron mass. In the ionosphere the peak plasma frequency is in the lower HF range of frequencies (3-10 MHz). The simplest model of the ionosphere is that of a plane-stratified plasma, where n is linearly related to altitude, denoted z, and independent of the horizontal coordinate:

$$\omega_p^2(\mathbf{r}) = \omega_{p0}^2 \frac{z}{z_0}. \tag{3}$$

Here we define $z = 0$ as the bottom of the ionosphere, which is typically about 200 km above the ground.

Now consider a radar pulse obliquely incident on the ionosphere at $z = 0$. The Cartesian components of the wavenumber at $z = 0$ can be written as

$$k_x = k \cos\theta \tag{4}$$

$$k_y = 0 \tag{5}$$

$$k_z = k \sin\theta, \tag{6}$$

where k is the wavenumber given by Equation (1), θ is the elevation angle, and the trajectory is assumed to lie in the x-z plane. Since the index of refraction, given by Equation (1), is only a function of z, the horizontal component of the wavenumber

k_x remains constant as the radar pulse propagates through the ionosphere. Therefore k_x maintains its freespace ($z = 0$) value:

$$k_x = \frac{\omega}{c} \cos\theta. \tag{7}$$

The value of k_z in the ionosphere is given by

$$\begin{aligned} k_z^2 &= k^2 - k_x^2 \\ &= \frac{\omega^2}{c^2} \sin^2\theta - \frac{\omega_{p0}^2}{c^2} \frac{z}{z_0}. \end{aligned} \tag{8}$$

The ratio k_z/k_x is the slope of the pulse trajectory $(x, 0, z)$ in the ionosphere:

$$\frac{k_z}{k_x} = \frac{dz}{dx} = \pm\sqrt{\tan^2\theta - \frac{\omega_{p0}^2}{\omega^2} \frac{z}{z_0} \sec^2\theta}. \tag{9}$$

By direct substitution into the previous formula, it can be shown that the pulse trajectory (or "ray") has the form of a parabola:

$$\frac{z}{z_0} = -\frac{\omega_{p0}^2}{4\omega^2} \sec^2\theta \left(\frac{x}{z_0}\right)^2 + \frac{\omega^2}{\omega_{p0}^2} \sin^2\theta. \tag{10}$$

This relation is drawn out in Figure 1. The origin of coordinates is denoted $(0, 0, 0)$, and the $z = 0$ and $x = 0$ intercepts of the pulse trajectory are shown by arrows.

2.2 Elevation Angle Resolution

The maximum penetration distance into the ionosphere occurs at the peak of the parabolic trajectory given by Equation (10):

$$z = \frac{\omega^2}{\omega_{p0}^2} z_0 \sin^2\theta. \tag{11}$$

We note that this distance is proportional to ω^2. Thus wideband radar pulses will disperse (or spread) in altitude. If the bandwidth of the signal is $\Delta\omega$, then it follows from Equation (11) that the spread in altitude is given by

$$\begin{aligned} \Delta z &= z(\omega + \Delta\omega) - z(\omega) \\ &\approx \frac{2\omega\Delta\omega}{\omega_{p0}^2} z_0 \sin^2\theta. \end{aligned} \tag{12}$$

When the transmitted beam is at low elevation angle, this spread in altitude can be interpreted as a spreading in elevation angle.

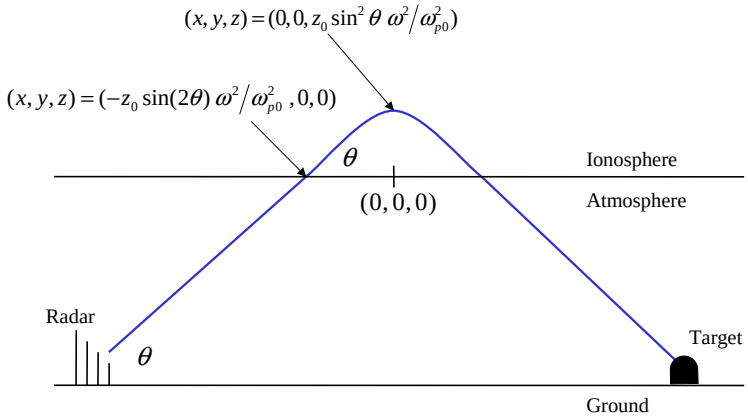

Figure 1: *Radar pulse trajectory.*

Let us consider the example $\omega/(2\pi) = 10$ MHz, $\omega_{p0}/(2\pi) = 3$ MHz, $\Delta\omega/(2\pi) = 100$ kHz, $z_0 = 50$ km, and $\theta = 15$ degrees. Even a rather large bandwidth of 100 kHz produces a spreading in elevation of about 700 m, which is an elevation angle spread of 0.04 degrees at 1000-km range.

Practical radar systems do not have the aperture to achieve an elevation resolution of 0.04 degrees. The largest existing sky wave radar systems [7, 8] have linear apertures on the order of 3 km, which could produce 2-degree resolution at 15-degree elevation if the radar beam could be steered in the endfire direction. A 2-degree beam at 1000-km range corresponds to a resolution cell of height 35 km. If clutter-producing irregularities are confined to the bottomside of the ionosphere, which is assumed above to be 50 km in extent, then the 2-degree beam encloses most of the vertical extent of the clutter.

2.3 Range Resolution

Limits exist on the bandwidth $\Delta\omega$ because of the elevation spreading computed in the previous section. Consider Figure 1. Let us denote the ground distance between the radar and the target as R and the distance between the ground and the peak

altitude of the pulse trajectory as h. The relation between R and h is given by

$$R \approx 2h \cot\theta. \tag{13}$$

In the previous section we computed the reflection height spread of a wideband pulse and called it Δz. This Δz produces a corresponding ΔR given by

$$\begin{aligned} \Delta R &= 2\Delta z \cot\theta \\ &= \frac{2\omega\Delta\omega}{\omega_{p0}^2} z_0 \sin(2\theta). \end{aligned} \tag{14}$$

If ΔR is larger than the intrinsic radar resolution $\pi c/\Delta\omega$, then target smearing will occur. So the limit on bandwidth is given by

$$\Delta R = \pi c/\Delta\omega, \tag{15}$$

which implies a bandwidth limit of

$$\Delta\omega = \sqrt{\frac{\pi c\omega_{p0}^2}{2\omega z_0 \sin(2\theta)}}. \tag{16}$$

For example, let us consider $\omega/(2\pi) = 10$ MHz, $\omega_{p0}/(2\pi) = 3$ MHz, $z_0 = 50$ km, and $\theta = 15$ degrees. The limit on bandwidth is $\Delta\omega/(2\pi) = 50$ kHz. It should be noted that lower elevation angles, sharper ionospheric layers (smaller z_0), and denser ionospheres (greater ω_{p0}) will allow an increase in the bandwidth limit.

3 Resolution In Azimuth Angle and Doppler

This chapter determines lower limits on the azimuth and Doppler resolution of an HF radar. Since the quiescent ionosphere is indistinguishable in the azimuth and Doppler radar dimensions, resolving power in these dimensions is limited only by the presence of fine-scale irregular ionospheric structure. This irregular structure manifests in distortions to the planar wavefronts of signals from the transmitter and echoes from targets. These distortions consist of random phase scintillations whose statistics relate to the expected spreading of the radar signal in the azimuth and Doppler dimensions [9, 10].

3.1 Perturbation of Wavefront Phase

A radar pulse propagates in the ionosphere following the dispersion relation of Equation (1) and the ray path of Equation (10). The phase along any part of the path is

$$\phi = \int ds\ k(\mathbf{r}). \tag{17}$$

where $k(\mathbf{r})$ is the pulse wavenumber, ds is an element of arc length, and $\mathbf{r} = (x, 0, z)$ is a point on the ray trajectory, as shown in Figure 2. Note that the trajectory is

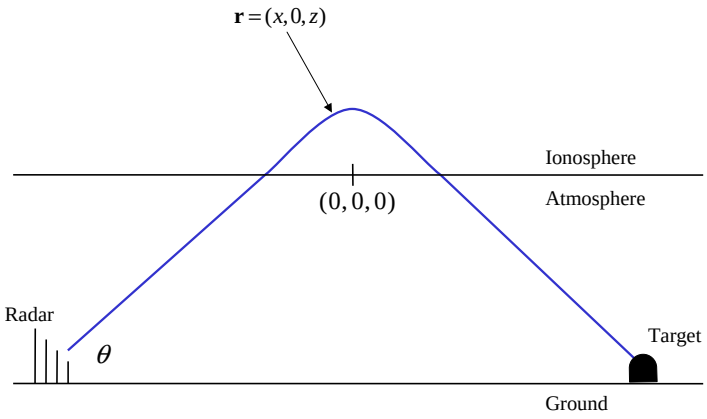

Figure 2: *Point* $\mathbf{r}$ *on signal trajectory.*

assumed to lie in the x-z plane.

Let us consider small-amplitude irregularities in the ionospheric plasma, such that the total ionospheric plasma density is $n = n_0 + n_1$, where n_0 is the quiescent plasma density and n_1 is the irregularity. The first-order Taylor-series perturbation to ϕ is given by

$$\phi_1 = \int ds\ n_1(\mathbf{r}) \frac{\partial k(\mathbf{r})}{\partial n}. \tag{18}$$

From Equation (1) we can compute the derivative of $k(\mathbf{r})$ with respect to density:

$$\frac{\partial k(\mathbf{r})}{\partial n} = -\frac{e^2}{2\epsilon_0 m\omega c\sqrt{1-\omega_p^2(\mathbf{r})/\omega^2}}. \tag{19}$$

From Equation (9) the element of arc length ds is given by

$$\begin{aligned} ds &= dx\ \sqrt{1+\left(\frac{dz}{dx}\right)^2} \\ &= dx\ \ \sec\theta\sqrt{1-\frac{\omega_p^2(\mathbf{r})}{\omega^2}}. \end{aligned} \tag{20}$$

Combining the previous three equations, we find that

$$\phi_1 = -r_e\lambda\sec\theta\int dx\ n_1(\mathbf{r}(x)), \tag{21}$$

where $r_e = e^2/(4\pi\epsilon_0 mc^2)$ is the classical electron radius (2.8×10^{-15} m) and λ is the freespace radar wavelength. The density n_1 is evaluated at point $\mathbf{r}$ which is parameterized by the x coordinate. Note that the irregularities have no effect on the shape of the ray path to first order. By Fermat's principle, the ray path comprises the path of minimum signal phase, and so path perturbations are second order in density perturbation [10].

We now imagine sampling ϕ_1 for a plane wave that has passed through the ionosphere, as shown in Figure 3. The sampled phases correspond to integrals over closely-spaced ray paths. The correlation is given by

$$\begin{aligned} R_{\phi_1}(\mathbf{R},T) &= \left\langle \left[-r_e\lambda\sec\theta\int dx\, n_1(\mathbf{r}(x),t)\right]\left[-r_e\lambda\sec\theta\int dx\, n_1(\mathbf{r}(x)+\mathbf{R},t+T)\right]\right\rangle \\ &\approx (r_e\lambda\sec\theta)^2\iint dx'\,dx''R_{n_1}(\mathbf{r}(x'')+\mathbf{R}-\mathbf{r}(x'),t(x'')+T-t(x')), \end{aligned} \tag{22}$$

where the angle brackets denote an average over all realizations of the argument and R_{n_1} is the autocorrelation function of the ionospheric irregularities. The density

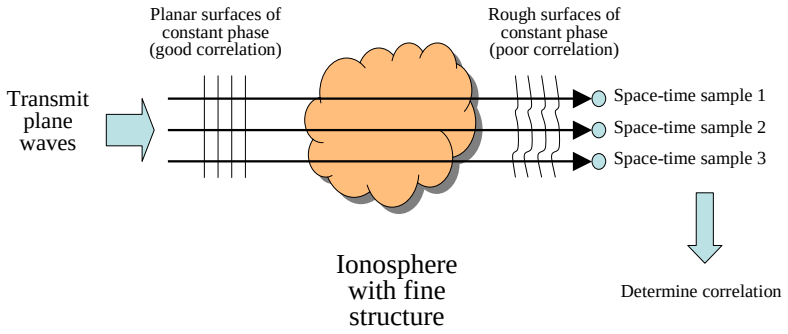

Figure 3: *Correlation of nearby signal paths.*

irregularities are now assumed to have fine-scale temporal dependence. However, we will make no attempt to account for a possible variation in the mean-square amplitude of the irregularities with altitude. A uniform distribution is assumed for simplicity. Taking Fourier transforms of both sides of Equation (22), we find that

$$S_{\phi_1}(\boldsymbol{\kappa},\Omega) = (r_e\lambda\sec\theta)^2 S_{n_1}(\boldsymbol{\kappa},\Omega)\iint dx'dx''\, e^{i\boldsymbol{\kappa}\cdot[\mathbf{r}(x'')-\mathbf{r}(x')]-i\Omega[t(x'')-t(x')]}. \tag{23}$$

where S_{ϕ_1} is the spectrum of ϕ_1, and S_{n_1} is the spectrum of n_1. We assume that the Doppler frequencies of interest (a few Hz) are small enough such that we can ignore $\Omega t \sim 10^{-2}$ compared with $\boldsymbol{\kappa}\cdot\mathbf{r} \geq 10^1$. We will also assume that the highly conducting magnetic field lines of the earth tend to stretch the plasma structure so that there is no variation in n_1 along the field lines. In the polar region, the field lines are also close to vertical. Thus, the phase variation $\kappa_z z \sim 10^{-1}$ can be neglected compared to $\kappa_x x \geq 10^1$. With these approximations, we can compute the integral as follows:

$$\begin{aligned} S_{\phi_1}(\boldsymbol{\kappa},\Omega) &\approx (r_e\lambda\sec\theta)^2 S_{n_1}(\boldsymbol{\kappa},\Omega)\iint dx'dx''\, e^{i\kappa_x(x''-x')} \\ &\approx 2\pi L(r_e\lambda\sec\theta)^2\delta(\kappa_x)S_{n_1}(\boldsymbol{\kappa},\Omega), \end{aligned} \tag{24}$$

where L is the horizontal distance travelled in the ionosphere.

3.2 Azimuth Angle Resolution

To find the azimuth resolution, we ignore temporal variations in S_{ϕ_1} in Equation (24). Furthermore, as remarked above, we can also ignore structure in z due to the highly conducting vertical magnetic field lines. We choose a two-dimensional power spectrum for n_1 that lies in the horizontal (κ_x, κ_y) plane [4, 11]:

$$S_{n_1}(\kappa_x, \kappa_y) = \frac{2\pi \langle n_1^2 \rangle}{\kappa_0^2 \left(1 + \kappa_x^2/\kappa_0^2 + \kappa_y^2/\kappa_0^2\right)^{3/2}}, \tag{25}$$

where $\kappa_0 \approx 10^{-4}$ m^{-1} [3] is the so-called outer scale length of irregularities and the spectrum is normalized such that its area is the mean-square density of the plasma irregularities n_1, namely $\langle n_1^2 \rangle = (2\pi)^{-2} \int d\kappa_x d\kappa_y \, S_{n_1}(\kappa_x, \kappa_y)$. Using Equation (24), we find

$$S_{\phi_1}(\kappa_y) = \frac{2\pi L \langle n_1^2 \rangle (r_e \lambda \sec\theta)^2}{\kappa_0^2 \left(1 + \kappa_y^2/\kappa_0^2\right)^{3/2}}. \tag{26}$$

The autocorrelation along the array is given by the inverse Fourier transform, which is given by Equation (9.6.25) in [12]:

$$\begin{aligned} R_{\phi_1}(Y) &= \frac{2\pi L \langle n_1^2 \rangle (r_e \lambda \sec\theta)^2}{\kappa_0^2} \frac{1}{2\pi} \int \frac{d\kappa_y \, e^{i\kappa_y Y}}{\left(1 + \kappa_y^2/\kappa_0^2\right)^{3/2}} \\ &= \left\langle \phi_1^2 \right\rangle \kappa_0 |Y| K_1(\kappa_0 |Y|), \end{aligned} \tag{27}$$

where K_1 is a modified Bessel function of the second kind. The correlation coefficient $\kappa_0 |Y| K_1(\kappa_0 |Y|)$ is plotted in Figure 4.

The mean-square value of ϕ_1 is

$$\left\langle \phi_1^2 \right\rangle = \frac{2L \langle n_1^2 \rangle (r_e \lambda \sec\theta)^2}{\kappa_0}. \tag{28}$$

As an example, let us consider $L = 600$ km, $\lambda = 30$ m, $\theta = 15$ deg, and $\langle n_1^2 \rangle = 10^{18}$ m^{-6}, which represents 1-percent density fluctuations of a peak ionosphere density of 10^{11} m^{-3}. This gives us a root-mean-square phase fluctuation $\sqrt{\langle \phi_1^2 \rangle}$ of about 10 radians.

Unfortunately, radars do not measure the phase ϕ_1 directly. Rather, they measure a complex signal amplitude $A = e^{i\phi_1}$. The autocorrelation of the complex signal amplitude A can be related to the autocorrelation of the phase ϕ_1 by [13]

$$R_A(Y) = \left\langle e^{-i\phi_1(y)} e^{i\phi_1(y+Y)} \right\rangle = e^{R_{\phi_1}(Y) - \left\langle \phi_1^2 \right\rangle}. \tag{29}$$

The complex amplitude autocorrelation function is

$$R_A(Y) = e^{-\left\langle \phi_1^2 \right\rangle [1 - \kappa_0 |Y| K_1(\kappa_0 |Y|)]}. \tag{30}$$

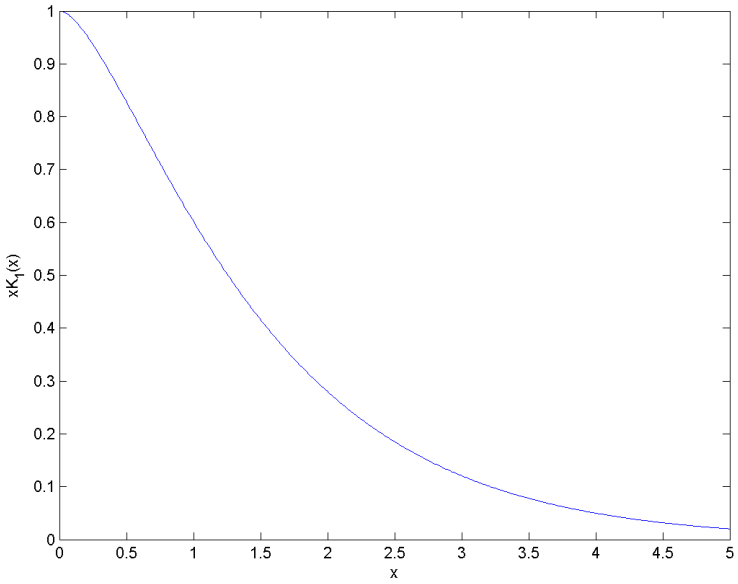

Figure 4: *Function* $xK_1(x)$.

R_A drops to a value of 0.5 when $\kappa_0 Y \approx 0.06$. With $\kappa_0 = 10^{-4}$ m^{-1}, this corresponds to a correlation length of about 600 m. Since the correlation function and wavenumber spectrum are Fourier transforms, the wavenumber spectrum S_A drops to a value of 0.5 at $\kappa_y \approx 1.6 \times 10^{-3}$ m^{-1}. Thus the spread in κ_y is $\Delta\kappa_y = 3.2 \times 10^{-3}$ m^{-1}. At 10 MHz, the radar radial wavenumber is $k = 0.21$ m^{-1}, so the minimum realizable azimuth resolution is $\Delta\phi = \Delta\kappa_y / k \approx 1$ degree.

3.3 Doppler Resolution

For the purpose of computing Doppler resolution, we assume that temporal fluctuations at a fixed point in space are due to the drifting motion of spatial structures, referred to as the Taylor hypothesis [10]. In other words, S_{n_1} can be written as

$$S_{n_1}(\boldsymbol{\kappa}, \Omega) = 2\pi S_{n_1}(\boldsymbol{\kappa}) \delta(\Omega - \boldsymbol{\kappa} \cdot \mathbf{v}_d), \tag{31}$$

where $\mathbf{v}_d$ is the plasma drift velocity. In the polar ionosphere, the convection of plasma is in the horizontal direction [14], so the z component of $\mathbf{v}_d$ is zero. If we insert the previous equation into Equation (24) we find that

$$S_{\phi_1}(\boldsymbol{\kappa}, \Omega) = 4\pi^2 L (r_e \lambda \sec\theta)^2 \delta(\kappa_x) S_{n_1}(\boldsymbol{\kappa}) \delta(\Omega - \kappa_x v_{dx} - \kappa_y v_{dy}). \tag{32}$$

If we take Equation (25) to represent S_{n_1}, then there is no dependence on κ_z on the right side. The two delta functions on the right side also remove the κ_x and Ω

coordinates, so we find

$$S_{\phi_1}(\Omega) = \frac{1}{v_{dy}} S_{\phi_1}(\kappa_y)\Big|_{\kappa_y=\Omega/v_{dy}}. \tag{33}$$

Thus the development in the previous section can be repeated, with κ_y replaced by Ω/v_{dy}. However, it is interesting to note that the Doppler spreading is due to motions tangential to the radar beam (y) as opposed to line of sight (x).

By examining the previous section, we can jump to the final result. The Doppler spread is

$$\Delta f = \frac{\Delta\kappa_y \, v_{dy}}{2\pi} \approx 5 \times 10^{-4} \, v_{dy} \text{ Hz}, \tag{34}$$

where we have taken $\Delta\kappa_y \approx 3.2 \times 10^{-3}$ m^{-1} at 10 MHz operation. The drift velocity v_{dy} can vary, so we choose a representative value of 100 m/s [4], which would imply a Doppler spread of 0.05 Hz, which would in turn allow integration times of about 20 seconds.

4 Auroral Clutter Radar Cross Section

We consider an auroral HF skywave radar whose purpose is to detect, locate, and track air targets over the interior of Canada. This scenario involves the detection of a moving point target against a background of auroral radar clutter. This section determines the RCS of auroral clutter and compares it to measured values.

Auroral radar clutter arises from scattering of radar signals by electrons in the auroral plasma, usually denoted as Thomson scatter. In an unstructured thermal ionospheric plasma, Thomson scatter observations generally require radars with a power-aperture product on the order of 10^{10} W-m^2 [15]. However, if there is macroscopic structuring in the plasma at scale lengths of one-half the radar wavelength, then the Thomson scatter can be enhanced by a Bragg scattering mechanism, and can be detected by radars with far smaller power-aperture products [16].

4.1 Thomson Scattering

In the HF band (3-30 MHz) we assume the plasma response to an incident electric field is dominated by electrons, as the ions have too much inertia to move appreciably. The conservation of momentum for an electron can be expressed as:

$$m\frac{d\mathbf{v}}{dt} = -e(\mathbf{E} + \mathbf{v} \times \mathbf{B}). \tag{35}$$

Here, m is the electron momentum, $\mathbf{v}$ is the electron velocity, $\mathbf{E}$ is the imposed electric field of the radar pulse, and $\mathbf{B}$ is the magnetic field of the earth. If we analyze $\mathbf{v}$ and $\mathbf{E}$ into Cartesian components and assume they have a time-harmonic $\exp(-i\omega t)$ amplitude, and orient the magnetic field $\mathbf{B}$ in the z direction, then it can be shown that

$$v_x = -\frac{ie}{m\omega}\frac{[E_x - i(\omega_c/\omega)E_y]}{1-(\omega_c/\omega)^2} \tag{36}$$

$$v_y = -\frac{ie}{m\omega}\frac{[E_y + i(\omega_c/\omega)E_x]}{1-(\omega_c/\omega)^2} \tag{37}$$

$$v_z = -\frac{ie}{m\omega}E_z, \tag{38}$$

where $\omega_c = eB/m$ is the so-called electron cyclotron frequency.

For simplicity, we consider radar frequencies $\omega \gg \omega_c$ such that we can ignore terms of order ω_c/ω. This means that in response to an applied electric field, the electrons quiver at a velocity given by

$$\mathbf{v}(\mathbf{r}) = -\frac{ie\mathbf{E}_0}{m\omega}e^{i\mathbf{k}_0\cdot\mathbf{r}}, \tag{39}$$

where $\mathbf{E}_0$ is the vector amplitude of the incident electric field of the radar pulse, $\mathbf{k}_0$ is the incident wavenumber, and $\mathbf{r}$ is a spatial co-ordinate with respect to the radar transmitter. The local current density is

$$\begin{aligned}\mathbf{J}(\mathbf{r}) &= -en(\mathbf{r})\mathbf{v}(\mathbf{r}) \\ &= n(\mathbf{r})\frac{ie^2\mathbf{E}_0}{m\omega}e^{i\mathbf{k}_0\cdot\mathbf{r}},\end{aligned} \tag{40}$$

where n is the electron density per unit volume. The vector potential at the radar receiver is given by

$$\begin{aligned}\mathbf{A} &= \int d\mathbf{r}'\,\frac{\mu_0\mathbf{J}(\mathbf{r}')}{4\pi||\mathbf{d}-\mathbf{r}'||}e^{ik_s||\mathbf{d}-\mathbf{r}'||} \\ &\approx \frac{\mu_0}{4\pi d}e^{ik_s d}\int d\mathbf{r}'\,\mathbf{J}(\mathbf{r}')e^{-i\mathbf{k}_s\cdot\mathbf{r}'} \\ &\approx \frac{i\mu_0 e^2\mathbf{E}_0}{4\pi dm\omega}e^{ik_s d}\int d\mathbf{r}'\,n(\mathbf{r}')e^{-i(\mathbf{k}_s-\mathbf{k}_0)\cdot\mathbf{r}'},\end{aligned} \tag{41}$$

where μ_0 is the permeability of free space, $\mathbf{d}$ is the displacement between the center of the radar resolution cell and the radar receiver, $\mathbf{k}_s$ is the scattered wavenumber, and the integration over $\mathbf{r}'$ denotes the region within the radar resolution cell. We make the usual assumption that this cell is in the radar far field (i.e. $||\mathbf{r}'|| \ll ||\mathbf{d}||$).

In the case of backscatter, we can take $\mathbf{k}_s = -\mathbf{k}_0$. The scattered field measured at the receiver is

$$\begin{aligned}\mathbf{E} &= \frac{\nabla\times\nabla\times\mathbf{A}}{-i\omega\mu_0\epsilon_0} \\ &\approx -\frac{i\omega}{k_s^2}\,\mathbf{k}_s\times(\mathbf{k}_s\times\mathbf{A}) \\ &= -\frac{\mathbf{E}_0}{d}\left(\frac{e^2}{4\pi\epsilon_0 mc^2}\right)e^{ik_s d}\int d\mathbf{r}'\,n(\mathbf{r}')e^{2i\mathbf{k}_0\cdot\mathbf{r}'} \\ &= -\frac{\mathbf{E}_0 r_e}{d}e^{ik_s d}\int d\mathbf{r}'\,n(\mathbf{r}')e^{2i\mathbf{k}_0\cdot\mathbf{r}'},\end{aligned} \tag{42}$$

where ϵ_0 is the permittivity of free space, c is the speed of light, and r_e is the classical electron radius (2.8×10^{-15} m).

We now consider the plasma density $n(\mathbf{r}')$ to be a random quantity, so that the received field $\mathbf{E}$ is also a random quantity. The mean-square field is:

$$\left\langle||\mathbf{E}||^2\right\rangle = \frac{||\mathbf{E}_0||^2 r_e^2}{d^2}\iint d\mathbf{r}_1'\,d\mathbf{r}_2'\,\left\langle n(\mathbf{r}_1')n^*(\mathbf{r}_2')\right\rangle e^{2i\mathbf{k}_0\cdot(\mathbf{r}_1'-\mathbf{r}_2')}, \tag{43}$$

where angle brackets denote an average of all realizations of the argument. If the correlation length of n is small compared to the radius of the volume over which the average is computed, then we can write the mean-square radiated field as

$$\begin{aligned}\left\langle ||\mathbf{E}||^2 \right\rangle &\approx \frac{||\mathbf{E}_0||^2 r_e^2}{d^2} \int d\mathbf{r}'_1 \, R_n(\mathbf{r}'_1) \, e^{2i\mathbf{k}_0 \cdot \mathbf{r}'_1} \int d\mathbf{r}'_2 \\ &\approx \frac{||\mathbf{E}_0||^2 r_e^2 V}{d^2} S(-2\mathbf{k}_0), \end{aligned} \tag{44}$$

where R_n is the plasma autocorrelation function, V is the volume of the region illuminated by the radar, and S is a power spectrum of the density irregularities.

The volumetric RCS is the RCS of perfectly conducting spheres per unit volume that would lead to the observed radiation intensity in a given direction. This is given as [15, 16]:

$$\begin{aligned}\sigma &= \frac{4\pi d^2 \left\langle ||\mathbf{E}||^2 \right\rangle}{V ||\mathbf{E}_0||^2} \\ &= 4\pi r_e^2 S(-2\mathbf{k}_0). \end{aligned} \tag{45}$$

The interpretation of this expression is that the total volumetric RCS is equal to the RCS of a single electron (the Thomson RCS $4\pi r_e^2$), times a factor S representing the enhancement due to Bragg scattering by the electron ensemble.

4.2 Determination of Radar Cross Section

In the above expression for σ, S is evaluated at a discrete wavenumber, which requires a three-dimensional non-singular power spectrum for n_1. We use a power spectrum given by [10, 17]:

$$S(\boldsymbol{\kappa}) = \frac{8\pi \left\langle n_1^2 \right\rangle}{\kappa_0^2 \kappa_{0z} (1 + \kappa_x^2/\kappa_0^2 + \kappa_y^2/\kappa_0^2 + \kappa_z^2/\kappa_{z0}^2)^2}. \tag{46}$$

This is an extension of the two-dimensional power spectrum given by Equation (25) to three dimensions to model non-singular behaviour in the direction of the magnetic field (assumed to be in the vertical z direction). Here, κ_{z0} is the outer wavenumber in the field-aligned direction, which we take as $\kappa_{0z} = 3 \times 10^{-8}$ m^{-1}, which is discussed at Equation (13) in [3]. If we assume $\left\langle n_1^2 \right\rangle = 10^{18}$ m^{-6} and $\kappa_0 = 10^{-4}$ m^{-1} as in the previous section, and assume 10 MHz radar operation such that $\mathbf{k}_0 \approx 0.21\hat{\mathbf{x}}$ m^{-1}, then we find that

$$\sigma = -75.7 \text{ dB}(\text{m}^2/\text{m}^3). \tag{47}$$

This value compares favorably to the result of an experimental determination in [2], which cites a mean value of -77.5 dB(m^2/m^3) observed in the Polar Fox II experiments.

5 Signal Processing

Reviewing the results from Chapters 2 and 3, we consider a resolution cell that has the following minimum dimensions at a nominal radar carrier frequency of 10 MHz and bandwidth of 10 kHz:

$$\begin{aligned} \text{Range} &= 15 \text{ km} \\ \text{Azimuth} &= 1 \text{ deg} \\ \text{Elevation} &= 2 \text{ deg} \\ \text{Doppler} &= 0.05 \text{ Hz} \end{aligned}$$

The three-dimensional volume of this cell is about 10^{13} m^3 at 1000-km range, or 130 dB relative to 1 m^3. Based on an aurora RCS of -77.5 $dB(m^2/m^3)$ from Chapter 4, the total RCS of the clutter is expected to be 52.5 dBm^2. Since the clutter arises from a large-scale ionospheric convection pattern, it is expected that in each 0.05-Hz Doppler cell, the ionospheric clutter is confined to a small range of azimuth angles, as per Equation (31). This range can be no smaller than the radar azimuth resolving limit of 1 degree. For simplicity of calculation, we will assume that this range is in fact 1 degree, such that the entire 52.5-dBm^2 clutter return is confined to a single 0.05-Hz Doppler cell.

We consider a target echo consisting of a plane wave of amplitude x that is received by a linear array of antenna elements spaced 0.5λ apart. The amplitude and phase response of the individual sensors to the plane wave is captured by an array manifold vector $\mathbf{v}$:

$$\mathbf{v}^H = \left[\begin{array}{cccc} 1 & e^{-i\pi \sin\varphi} & e^{-2i\pi \sin\varphi} & \dots \end{array} \right], \tag{48}$$

where H denotes conjugate transpose, and φ is the azimuthal angle of propagation of the plane wave with respect to the array boresight.

In addition to the plane wave signal, the sensors are corrupted by a "noise" vector $\mathbf{n}$ that is dominated by an auroral clutter signal. The noise $\mathbf{n}$ is a random vector where each element represents the clutter received at each sensor. For analytic tractability, we abandon the detailed autocorrelation calculations of the previous chapters and assume a simple exponential correlation function:

$$R_A(Y) = e^{-|Y|/L}, \tag{49}$$

where Y is the lag along the array and L is the signal correlation length along the array. The exponential drops off somewhat more rapidly than the Bessel correlation function derived in Chapter 3, so the results given in this chapter may ultimately underestimate the capabilities of adaptive processing schemes. If the intersensor

spacing is d, and we define $\rho = \exp(-d/L)$, then a sensor covariance matrix can be written:

$$\mathbf{R}_n = \sigma_n^2 \begin{bmatrix} 1 & \rho & \rho^2 & \\ \rho & 1 & \rho & \\ \rho^2 & \rho & 1 & \\ & & & \ddots \end{bmatrix}, \tag{50}$$

where the variances of all of the elements of $\mathbf{n}$ are assumed to be equal to σ_n^2. The array measurement consists of the target vector plus the noise vector, which we write as a vector $\mathbf{y}$:

$$\mathbf{y} = \mathbf{v}x + \mathbf{n}. \tag{51}$$

We devise a linear estimator for x that consists of summing the measured signals according to a "weight" function $\mathbf{w}$. This estimator is denoted as

$$\hat{x} = \mathbf{w}^H \mathbf{y}. \tag{52}$$

In the next section, we look at a common technique for choosing $\mathbf{w}$.

5.1 Receive-Side Adaptive Processing

Adaptive processors can produce unbiased estimates as well as reduce the variance of the noise at the output. The minimum-variance distortionless response (MVDR) processor is optimal in this regard and consists of the weights [5]

$$\mathbf{w}^H = \frac{\mathbf{v}^H \mathbf{R}_n^{-1}}{\mathbf{v}^H \mathbf{R}_n^{-1} \mathbf{v}}. \tag{53}$$

Let us compute the signal-to-noise (SNR) improvement of this processor. From Equation (51), the input SNR is simply x^2/σ_n^2. The output SNR is given by

$$\begin{aligned} \frac{x^2}{\sigma_{\hat{x}}^2} &= \frac{x^2}{\langle (\hat{x} - \langle \hat{x} \rangle)(\hat{x} - \langle \hat{x} \rangle)^H \rangle} \\ &= x^2 \mathbf{v}^H \mathbf{R}_\mathbf{n}^{-1} \mathbf{v}. \end{aligned} \tag{54}$$

The SNR improvement of the processor is the ratio of output SNR to input SNR, which we denote as the array gain G:

$$G = \sigma_n^2 \mathbf{v}^H \mathbf{R}_n^{-1} \mathbf{v}. \tag{55}$$

By multiplication with $\mathbf{R}_n$, one can prove that $\mathbf{R}_n^{-1}$ is given by

$$\mathbf{R}_n^{-1} = \frac{1}{\sigma_n^2(1-\rho^2)} \begin{bmatrix} 1 & -\rho & 0 & 0 & & & \\ -\rho & 1+\rho^2 & -\rho & 0 & & & \\ 0 & -\rho & 1+\rho^2 & -\rho & & & \\ 0 & 0 & -\rho & 1+\rho^2 & & & \\ & & & & \ddots & & \\ & & & & & 1+\rho^2 & -\rho \\ & & & & & -\rho & 1 \end{bmatrix}. \tag{56}$$

Using the notation $u = e^{i\pi \sin\varphi}$, we find that

$$G = \frac{N + (N-2)\rho^2 - (N-1)(\rho u + \rho u^{-1})}{1-\rho^2}, \tag{57}$$

where N is the number of sensors. G is large when $u \approx -1$ and $\rho \approx 1$, in which case

$$G \approx \frac{2(N-1)}{1-\rho}. \tag{58}$$

It was determined in Chapter 3 that target signals are correlated a maximum of about 600 m along the array in auroral conditions. For 15-m sensor spacing (a fully sampled array at 10 MHz), $N = 40$ is therefore the largest useful number of sensors. The clutter is also subject to the same correlation length limitation. A correlation of 0.5 at 600 m linearly extrapolated to 15 m would suggest a clutter correlation coefficient of $\rho = 0.99$ between adjacent sensors. This means that G is at most 7,800 (38.9 dB). This would serve to reduce the 52.5-dBm^2 clutter return to 13.6 dBm^2, which is not sufficient to detect a 10-dBm^2 target. Thus, in the next section we consider combined transmit and receive adaptive processing to increase the clutter cancellation.

5.2 Transmit-Side Adaptive Processing

Here we consider combined transmit-side and receive-side adaptive processing. The estimation problem at each of N receive sensors can now be written as

$$\mathbf{y} = \mathbf{v}x + \mathbf{n}_1 + \mathbf{n}_2 + \ldots, \tag{59}$$

where the noise terms refer to the auroral clutter that is arriving from M transmit signals. We assume that the transmit waveforms are orthogonal, such that the matched filter receive system can distinguish the signals transmitted from the different transmit antennas. This orthogonality allows one to form linear combinations of the transmit waveforms and effectively form an adaptive transmit processor for each receive element. In other words, in the above equation, one cannot add the noise

terms since they are mutually correlated and must be individually accounted for by a description with MN degrees of freedom. The available degrees of freedom can be accounted for by forming a combined transmit-receive processor whose array manifold vector and noise covariance are the Kronecker products of the separate transmit and receive systems. If T denotes transmit, R denotes receive, and C denotes combined, then we have that

$$\mathbf{v}_C = \mathbf{v}_T \otimes \mathbf{v}_R \tag{60}$$

$$\mathbf{R}_{nC} = \mathbf{R}_{nT} \otimes \mathbf{R}_{nR}. \tag{61}$$

The array gain for the combined system is

$$\begin{aligned} G_C &= \sigma_{nC}^2 \mathbf{v}_C^H \mathbf{R}_{nC}^{-1} \mathbf{v}_C \\ &= \sigma_{nT}^2 \sigma_{nR}^2 (\mathbf{v}_T \otimes \mathbf{v}_R)^H (\mathbf{R}_{nT} \otimes \mathbf{R}_{nR})^{-1} (\mathbf{v}_T \otimes \mathbf{v}_R). \end{aligned} \tag{62}$$

The inverse of a Kronecker product is the Kronecker product of the inverses, and the Hermitian conjugate of a Kronecker product is the Kronecker product of the Hermitian conjugates, thus

$$G_C = \sigma_{nT}^2 \sigma_{nR}^2 (\mathbf{v}_T^H \otimes \mathbf{v}_R^H)(\mathbf{R}_{nT}^{-1} \otimes \mathbf{R}_{nR}^{-1})(\mathbf{v}_T \otimes \mathbf{v}_R). \tag{63}$$

Recognizing the identity

$$(\mathbf{A} \otimes \mathbf{B})(\mathbf{C} \otimes \mathbf{D}) = \mathbf{AC} \otimes \mathbf{BD}, \tag{64}$$

leads to

$$\begin{aligned} G_C &= \sigma_{nT}^2 \sigma_{nR}^2 (\mathbf{v}_T^H \mathbf{R}_{nT}^{-1} \otimes \mathbf{v}_R^H \mathbf{R}_{nR}^{-1})(\mathbf{v}_T \otimes \mathbf{v}_R) \\ &= (\sigma_{nT}^2 \mathbf{v}_T^H \mathbf{R}_{nT}^{-1} \mathbf{v}_T) \otimes (\sigma_{nR}^2 \mathbf{v}_R^H \mathbf{R}_{nR}^{-1} \mathbf{v}_R) \\ &= G_T G_R. \end{aligned} \tag{65}$$

Thus, the array gain of the combined system is simply equal to product of the array gains of the separate transmit and receive processors. For the combined adaptive processor it should be noted that under quasi-monostatic operation, the transmit and receive signal paths are similar, which would lead to a transmit array covariance similar to the receive array covariance. Thus the transmit processor improves performance by a factor of

$$G_T \approx \frac{2(M-1)}{1-\rho}. \tag{66}$$

A simple transmit processor of $M = 2$, for example, would increase the clutter cancellation capability of the radar by 23 dB. Combined with a $N = 40$ receive-side processor discussed above, this would reduce a 52.5-dBm^2 clutter source to -9.4 dBm^2, which would permit detection of small 10-dBm^2 targets.

While the principle of adaptive arrays has been illustrated above for beamforming in the azimuthal angular dimension φ, the same process could be used in the elevation dimension θ, since target signals for a given range gate generally arrive at a different elevation angle that those for the clutter signal. However, the elevation angle separation between target and clutter is generally small (i.e. $u \approx 1$), which severely limits the achievable array gain.

6 Conclusion

This memorandum has described some of the rudimentary considerations for operating an HF sky wave radar in the auroral zone. Chapter 2 looked at the simplest macroscopic model of the ionosphere and computed the elevation and range resolution of the radar. It was shown that the vertical inhomogeneity of the ionosphere causes a transmit beam to spread in elevation. This elevation spread is far less in extent than what can be resolved by practical radar systems and can be ignored. However, the vertical extent of clutter-producing irregularities is also on the order of the smallest resolution available from current radar systems. With regard to range resolution, the ionosphere causes wideband radar pulses to spread in ground range. If this ground range spreading exceeds the radar range resolution, then performance is degraded. This effect places practical limits on the radar waveform bandwidth.

Chapter 3 described the limits on the obtainable azimuth and Doppler resolution of an HF radar. These limits are imposed by the presence of plasma density irregularities in the ionospheric propagation path. It is found that for an assumption of 1-percent fluctuation levels in the propagation medium, the phase fronts incident on a linear array have a fluctuation level on the order of 10 radians and a correlation length of about 600 m along the array. This limits azimuth resolving capability to about 1 degree at 10 MHz. The limit on Doppler resolution is determined by invoking the Taylor hypothesis, which supposes that temporal variations in the ionosphere are due to drifting spatial structure. The Doppler spreading of a signal is therefore directly proportional to the drift speed of the structures. At a nominal drift rate of 100 m/s, the Doppler spreading is about 0.05 Hz, which is sufficient to support coherent integration times to about 20 seconds.

In Chapter 4, we briefly considered Thomson scattering from a structured plasma and compared theoretical values of auroral clutter RCS with experimentally deduced values. It is found that there is reasonable agreement with the experimental values in the case of 1-percent density fluctuations.

Chapter 5 looked at signal-to-clutter ratios using representative covariance matrices and concluded that small 10 to 20 dBm^2 RCS aircraft cannot be detected with receive-side-only adaptive processing. However, combining the adaptive receive array with even a small adaptive transmit array can dramatically improve the clutter cancellation to the point where small aircraft can be detected. The reason is that the total number of degrees of freedom in the combined processor is the product of the degrees of freedom in the individual receive and transmit processors. The calculations were carried out for the case of adaptive processing in azimuth angle. However, it is noted that adaptivity may also be implemented in elevation angle, although the physical configuration of a ground-based over-the-horizon radar gives inherently poor resolving capability in elevation angle, and resulting limited ability to cancel clutter

by exploiting adaptive processing in that dimension.

References

[1] Headrick, J. M. (1990). HF over-the-horizon radar. In M. I. Skolnik, (Ed.), *Radar handbook*, pp. 24.1–24.43. New York: McGraw-Hill.

[2] Elkins, T. J. (1980). A model for high frequency radar auroral clutter. (RADC-TR-80-122). Rome Air Development Center, Griffiss AFB, New York.

[3] Hysell, D. L., Kelley, M. C., Swartz, W. E., and Farley, D. T. (1994). VHF radar and rocket observations of equatorial spread F on Kwajalein. *Journal of Geophysical Research*, 99 (A8), 15065–15086.

[4] Vallieres, X., Villain, J.-P., Hanuise, C., Andre, R. (2004). Ionospheric propagation effects on spectral widths measured by SuperDARN HF radars. *Annales Geophysicae*, 22, 2023–2031.

[5] Capon, J. (1969). High-resolution frequency-wavenumber spectrum analysis. *Proceedings of the IEEE*, 57 (8), 1408–1418.

[6] Chen, F. F. (1984). Introduction to plasma physics and controlled fusion. 2nd ed. New York: Plenum Press.

[7] Colegrove, S. B. (2000). Project Jindalee: from bare bones to operational OTHR. In *Proceedings of the 2000 IEEE International Radar Conference*, 825–830. Alexandria, Virginia: Institute of Electrical and Electronics Engineers.

[8] Headrick, J. M. and Thomason, J. F. (1998). Applications of high-frequency radar. *Radio Science*, 33 (4), 1045–1054.

[9] Tatarskii, V. I. (1961). Wave propagation in a turbulent medium. New York: Dover.

[10] Coleman, C. J. (1996). A model of HF sky wave radar clutter. *Radio Science*, 31 (4), 869–875.

[11] Woodman, R. F. and Basu, S. (1978). Comparison between in situ measurements of F-region irregularities and backscatter observations at 3-m wavelength. *Geophysical Research Letters*, 5, 869–872.

[12] Abramowitz, M. and Stegun, I. A. (1964). Handbook of mathematical functions with formulas, graphs, and mathematical tables. New York: Dover, p. 370.

[13] Reed, I. S. (1962). On a moment theorem for complex Gaussian processes. *IRE Transactions on Information Theory*, 8 (4), 194–195.

[14] Kelley, M. C. (1989). The earth's ionosphere. San Diego: Academic Press, p. 151.

[15] Evans, J. V. (1969). Theory and practice of ionosphere study by Thomson scatter radar. *Proceedings of the IEEE*, 57 (4), 496–530.

[16] Booker, H. G. (1956). A theory of scattering by non-isotropic irregularities with application to radar reflections from the aurora. *Journal of Atmospheric and Terrestrial Physics*, 8, 204–221.

[17] Gherm, V. E., Zernov, N. N., and Strangeways, H. J. (2005). HF propagation in a wideband ionospheric fluctuating reflection channel: physically based software simulator of the channel. *Radio Science*, 40 (1), 1–15.

DOCUMENT CONTROL DATA

(Security classification of title, body of abstract and indexing annotation must be entered when the overall document is classified)

1. ORIGINATOR (the name and address of the organization preparing the document. Organizations for whom the document was prepared, e.g. Establishment sponsoring a contractor's report, or tasking agency, are entered in section 8.)

   Defence R&D Canada - Ottawa
   Ottawa, Ontario, K1A 0Z4

2. SECURITY CLASSIFICATION (overall security classification of the document, including special warning terms if applicable)

   UNCLASSIFIED

3. TITLE (the complete document title as indicated on the title page. Its classification should be indicated by the appropriate abbreviation (S,C or U) in parentheses after the title.)

   Detection of Aircraft by High Frequency Sky Wave Radar Under Auroral Clutter-Limited Conditions (U)

4. AUTHORS (Last name, first name, middle initial)

   Riddolls, Ryan J.

5. DATE OF PUBLICATION (month and year of publication of document)	6a. NO. OF PAGES (total containing information. Include Annexes, Appendices, etc.)	6b. NO. OF REFS (total cited in document)
March 2009	34	17

7. DESCRIPTIVE NOTES (the category of the document, e.g. technical report, technical note or memorandum. If appropriate, enter the type of report, e.g. interim, progress, summary, annual or final. Give the inclusive dates when a specific reporting period is covered.)

   Technical Memorandum

8. SPONSORING ACTIVITY (the name of the department project office or laboratory sponsoring the research and development. Include the address.)

   Defence R&D Canada - Ottawa
   Ottawa, Ontario, K1A 0Z4

9a. PROJECT OR GRANT NO. (if appropriate, the applicable research and development project or grant number under which the document was written. Please specify whether project or grant)	9b. CONTRACT NO. (if appropriate, the applicable number under which the document was written)
Project 13mc06	

10a. ORIGINATOR'S DOCUMENT NUMBER (the official document number by which the document is identified by the originating activity. This number must be unique to this document.)	10b. OTHER DOCUMENT NOS. (Any other numbers which may be assigned this document either by the originator or by the sponsor)
DRDC Ottawa TM 2008-336	

11. DOCUMENT AVAILABILITY (any limitations on further dissemination of the document, other than those imposed by security classification)

- (x) Unlimited distribution
- ( ) Distribution limited to defence departments and defence contractors; further distribution only as approved
- ( ) Distribution limited to defence departments and Canadian defence contractors; further distribution only as approved
- ( ) Distribution limited to government departments and agencies; further distribution only as approved
- ( ) Distribution limited to defence departments; further distribution only as approved
- ( ) Other (please specify):

12. DOCUMENT ANNOUNCEMENT (any limitation to the bibliographic announcement of this document. This will normally correspond to the Document Availability (11). However, where further distribution (beyond the audience specified in 11) is possible, a wider announcement audience may be selected.)

    Unlimited

13. ABSTRACT (a brief and factual summary of the document. It may also appear elsewhere in the body of the document itself. It is highly desirable that the abstract of classified documents be unclassified. Each paragraph of the abstract shall begin with an indication of the security classification of the information in the paragraph (unless the document itself is unclassified) represented as (S), (C), or (U). It is not necessary to include here abstracts in both official languages unless the text is bilingual).

This memorandum describes some of the rudimentary considerations for operating a high frequency sky wave radar in Canada for aircraft detection. A simple macroscopic model of the ionosphere is examined, and the elevation and range resolution limits of a high frequency radar are computed. Limits on azimuth and Doppler resolving capabilities of a radar arise from the presence of plasma density irregularities in the ionospheric propagation path. Scattering from the aurora is quantified using Thomson scattering theory and reasonable agreement with the experimental values of radar cross section can be found in the case of 1-percent plasma density fluctuations. However, the auroral scatter is sufficiently large to prevent detection of small aircraft with radar cross sections of 10 to 20 dBsm. Combining receive-side adaptive processing with adaptive elements on the transmit side allows the targets to be detected.

14. KEYWORDS, DESCRIPTORS or IDENTIFIERS (technically meaningful terms or short phrases that characterize a document and could be helpful in cataloguing the document. They should be selected so that no security classification is required. Identifiers such as equipment model designation, trade name, military project code name, geographic location may also be included. If possible keywords should be selected from a published thesaurus. e.g. Thesaurus of Engineering and Scientific Terms (TEST) and that thesaurus-identified. If it is not possible to select indexing terms which are Unclassified, the classification of each should be indicated as with the title.)

HIGH FREQUENCY
RADAR
OVER THE HORIZON
SKY WAVE
AURORA
RADIO
PROPAGATION
IONOSPHERE
PLASMA
IRREGULARITIES
CLUTTER
ANTENNA
ARRAY

Defence R&D Canada

Canada's leader in Defence
and National Security
Science and Technology

R & D pour la défense Canada

Chef de file au Canada en matière
de science et de technologie pour
la défense et la sécurité nationale

www.drdc-rddc.gc.ca